JOURNAL OF MATERIALS SCIENCE 29 (1994) 1867–1872

Effect of particle-size distribution on sintering

Part I *Modelling*

J.-M. TING*, R. Y. LIN
Department of Material Sciences and Engineering, University of Cincinnati, Cincinnati, OH 45219, USA

A sintering model, taking into account the effect of particle-size distribution and the effect of grain growth, has been derived. The model predicts a dependence of densification on the width of the particle-size distribution. This dependence is strongly affected by the occurrence of grain growth. Prior to the occurrence of grain growth, the model predicts that the densification rate increases and then decreases as the particle-size distribution width of the original powder increases. After grain growth occurs, the densification rate decreases as the particle-size distribution width of the starting powder increases.

1. Introduction

The changes of microstructures during sintering are influenced by a host of factors which are determined by the chemical and physical properties of the raw powders. The influence of chemistry, such as additives, has received wide attention. On the other hand, the effect of particle-size distribution on sintering has been not so well studied [1–4]. Investigations on comparing the sintering behaviour of powders with the same average size, but varying the size distribution width are limited.

It has been suggested that mono-sized powders are preferable in producing dense, uniform, fine-grained microstructures [5–10]. These results have encouraged the production of nearly mono-sized powders and, in addition, raised the question of how narrow a size distribution is required. This poses a question of the dependence of sintering kinetics on particle-size distribution.

An early theoretical work on the effect of particle size distribution was carried out by Coble [11]. The work focused on the densification in the initial stage of sintering. The diffusion model, for both lattice diffusion and grain-boundary diffusion, of the initial stage of sintering was developed. The model predicted that the sintering rates for binary mixtures were intermediate between the behaviour of the end-member sizes, and a 25% increase of sintering rate could be obtained when interstitial particles were introduced. Unfortunately, there are no experimental data to support this model. In addition, parameters characterizing particle-size distribution did not enter into the modelling. It thus becomes impractical in predicting the sintering kinetics of powders characterized by a common distribution function.

Recently, a model for both the initial and the intermediate stages of sintering was developed [2]. The model predicted a decrease in sintering rate as the particle-size distribution width increases for both the initial and the intermediate stage of sintering. This is apparently contrary to Coble's model and the model on bimodal powders [12]. Here, also, no experimental data are available to support this model. In fact, one can expect the benefit of adding finer powders to mono-sized powders because of the higher driving force provided by them.

The purpose of this study was to reinvestigate the effect of particle-size distribution on sintering kinetics. Both the initial stage and the later stages of sintering were investigated, and only lattice diffusion and boundary diffusion were included.

2. Background

In the past, a number of sintering models have been reported for both the initial stage of sintering [13–27] and the later stages of sintering [28–36]. The resulting equations can be summarized as follows. For the initial stage of sintering

$$\frac{\Delta L}{L_0} = \frac{K_1 D \gamma_s \Omega w}{G^m k T} t^n \quad (1)$$

where K_1 and w are constant, D is the diffusivity, γ_s is the surface energy, Ω is the atomic volume, G is the particle or grain size, k is the Boltzmann's constant, T is temperature, and m is a constant depending on the diffusion path. For the later stages of sintering

$$f(P) = K_2 \frac{\gamma_s \Omega D}{G^m k T} (t_f^n - t^n) \quad (2)$$

where $f(P)$ is a function of porosity P, K_2 is a constant, and t_f is the total sintering time. Most work [28–36] indicated that $f(P)$ is linearly proportional to P.

The above equations do not include the effect of grain growth. In fact, there are similarities between

* *Present address*: Applied Sciences, Inc., P.O. Box 579, Cedarville, OH 45314, USA.

models of the initial stage and the intermediate stage of sintering [35, 37]. In addition to the geometric similarity, the other similarities include transfer of matter from particles to adjacent pores through a similar mechanism prior to the occurrence of grain growth. In fact, both Equations 1 and 2 can be represented by [2]

$$R = K_3 \frac{t^n}{G^{m_0}} \tag{3}$$

where R denotes a general relative shrinkage at time t, m_0 is a constant depending on the diffusion path, and K_3 is a constant.

When grain growth occurs, Equation 3 is not applicable, in that the grain size is a function of time. Recently, sintering equations incorporating grain growth have been derived [38, 39]. The resulting equations can be expressed as

$$R(t) = K_4 \frac{G(t)}{G_0^{m_1}} \tag{4}$$

where R and G now depend on time, G_0 is the original particle size, K_4 is a constant, and m_1 depends on the diffusion path.

It can be seen that none of the above models takes into account the particle-size distribution. In the following, we will be incorporating the particle-size distribution into our sintering model.

3. The model

We first define a size-distribution function, $f(G)$, such that

$$\mathrm{d}v = f(G)\,\mathrm{d}G \tag{5}$$

$$\int f(G)\mathrm{d}G = 1 \tag{6}$$

where $\mathrm{d}v$ is the volume fraction of particles contained in $G + \mathrm{d}G$.

When shrinkage of a compact takes place, by combining Equations 3 and 5, the dimensional change of volume, $\mathrm{d}v$, becomes

$$\delta v = K_3 \frac{t^n}{G^{m_0}} f(G)\delta G \tag{7}$$

The total dimensional change can then be expressed as

$$\Delta v = \int K_3 \frac{t^n}{G^{m_0}} f(G)\delta G \tag{8}$$

As a result, the shrinkage of powder compact is

$$\begin{aligned} R &= \int K_3 \frac{t^n}{G^{m_0}} f(G)\mathrm{d}G \Big/ \int f(G)\mathrm{d}G \\ &= K_3 t^n F_0(G) \end{aligned} \tag{9}$$

where $F_0(G)$ denotes the shrinkage rate factor before the occurrence of grain growth and depends on the characteristics of the starting particle-size distribution. Equation 9 is applicable to the initial stage of sintering as well as to the intermediate stage of sintering prior to the occurrence of grain growth.

When grain growth occurs, the rate of densification may be obtained by taking the time derivative of Equation 4, i.e.

$$\frac{\mathrm{d}R}{\mathrm{d}t} = K_4 \frac{1}{G_0^{m_1}} \frac{\mathrm{d}}{\mathrm{d}t}[G(t)] \tag{10}$$

For poly-dispersed grains, the dependence of grain growth on time can be expressed as [40]

$$\frac{\mathrm{d}G}{\mathrm{d}t} = K_5 \left(\frac{1}{G_g} - \frac{1}{G} \right) \tag{11}$$

where G_g is the geometric mean size and K_5 is a constant. The above equation is applicable to grain growth in a single-phase system such as a dense body. However, it is used as an approximation in the current model for reasons to be discussed later. As a result, for powders characterized by some distribution function $f(G(t))$ (notice that the grain size is a function of time), the dimensional change of grains falls between G and $G + \delta G$ becomes

$$\delta v = \int K_6 \frac{1}{G_0^{m_1}} \left(\frac{1}{G_g} - \frac{1}{G} \right) f(G)\delta G\,\mathrm{d}t \tag{12}$$

where K_7 is a constant. To proceed with the modelling, it is assumed that grain growth is self-similar as in the normal grain growth [41]. The case where abnormal grain growth occurs will be discussed later. The assumption of self-similar grain growth would allow separation of variables to be applied to Equation 12. Therefore, Equation 12 becomes

$$\delta v = \int K_6 \frac{1}{G_0^{m_1}} \left(\frac{1}{G_{0,g}} - \frac{1}{G_0} \right) f(G_0)\delta G_0 h(t)\mathrm{d}t \tag{13}$$

where $h(t)$ is some function of t and related to the grain-growth coefficient. Consequently, integrating Equation 13 over the size and dividing the result by the original dimension, we have the shrinkage expressed as

$$\begin{aligned} R &= \iint K_6 \frac{1}{G_0^{m_1}} \left(\frac{1}{G_{0,g}} - \frac{1}{G_0} \right) f(G_0)h(t)\mathrm{d}G_0\mathrm{d}t \Big/ \\ &\quad \int f(G_0)\mathrm{d}G_0 \\ &= K_7 H(t) F_1(G_0) \end{aligned} \tag{14}$$

where G_0 in Equation 14 is the initial particle size and is independent of time, $f(G_0)$ characterizes the distribution of initial particle sizes, $H(t)$ is the integration of $h(t)$ over t, and $F_1(G_0)$ denotes the rate factor of shrinkage as grain growth occurs. The effect of particle-size distribution on sintering kinetics can be obtained from Equations 9 and 14 by performing integrations to obtain F_0 and F_1.

4. Results

In order to perform the integrations, the commonly used log-normal distribution is assumed for the powder system to be analysed. The numerical values of constants m_0 and m_1 used in the integration are given in Table 1. Only lattice diffusion and boundary diffusion are considered here. In cases of evaporation–condensation and surface diffusion, the constants listed in Table I need to be changed for modelling; and it will be seen later that similar results can be obtained

TABLE I The numerical values of constants m_0 and m_1 used in integrating Equations 9 and 14

	Boundary Diffusion	Lattice Diffusion
m_0 Before grain growth	8/3	3
m_1 Grain growth occurs	4	3

in spite of the difference in these constants. In the modelling, powders with three different mean sizes, i.e. $G_g = 0.5$, 1.0, and 2.0 μm and various particle-size distributions, were included.

Figs 1 and 2 plot the results for grain-boundary diffusion and lattice diffusion, respectively, before grain growth takes place. In all cases shown in these two figures, the rate factor increases and then decreases as the starting particle-size distribution width increases. On the other hand, as grain growth occurs, the rate factor, F_1, decreases as the starting particle-size distribution width increases. Figs 3 and 4 show such results for grain-boundary diffusion and lattice diffusion, respectively. In all the figures above, larger particle size reduces the rate factor.

5. Discussion

The model described above predicts a change of densification rate as a function of the initial particle-size distribution before grain growth occurs and as a

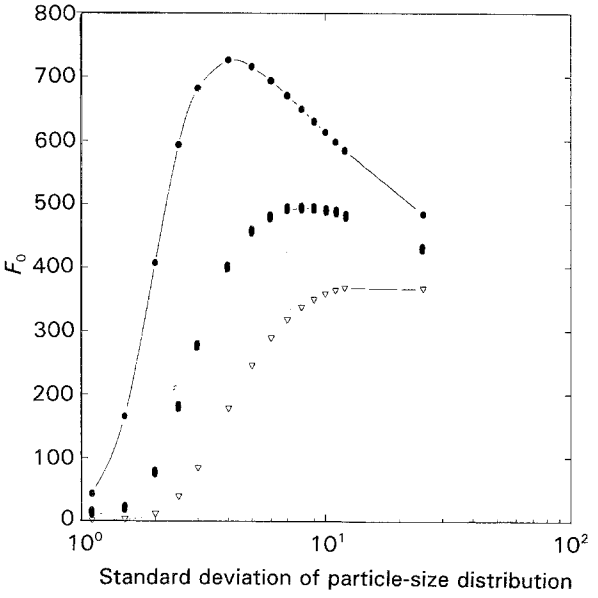

Figure 1 A plot showing the relationship between the rate factor, F_0, and the standard deviation prior to grain growth in the case of a lattice diffusion-controlled process. G_g: (●) 0.5 μm, (◖) 1.0 μm, (▽) 2.0 μm.

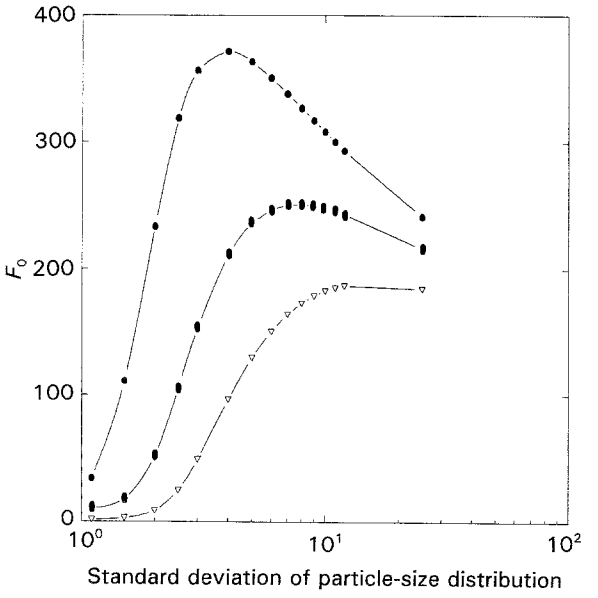

Figure 2 A plot showing the relationship between the rate factor, F_0, and the standard deviation prior to grain growth in the case of a boundary diffusion-controlled process. G_g: (●) 0.5 μm, (◖) 1.0 μm, (▽) 2.0 μm.

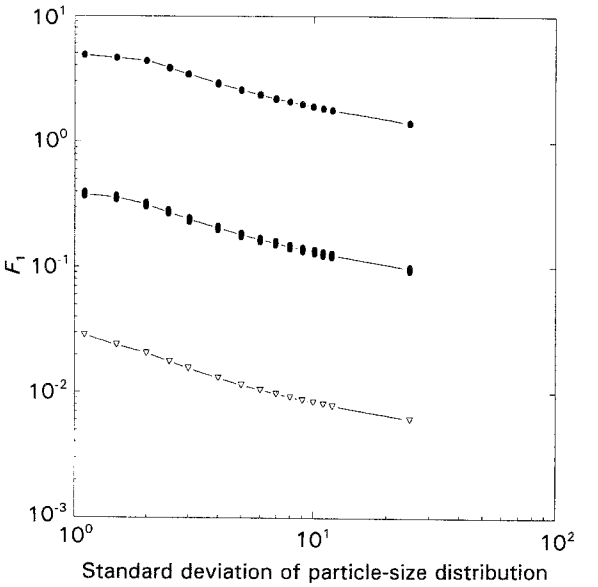

Figure 3 When grain growth occurs (in lattice diffusion-controlled process), the rate factor, F_1, decreases when the standard deviation decreases. G_g: (●) 0.5 μm, (◖) 1.0 μm, (▽) 2.0 μm.

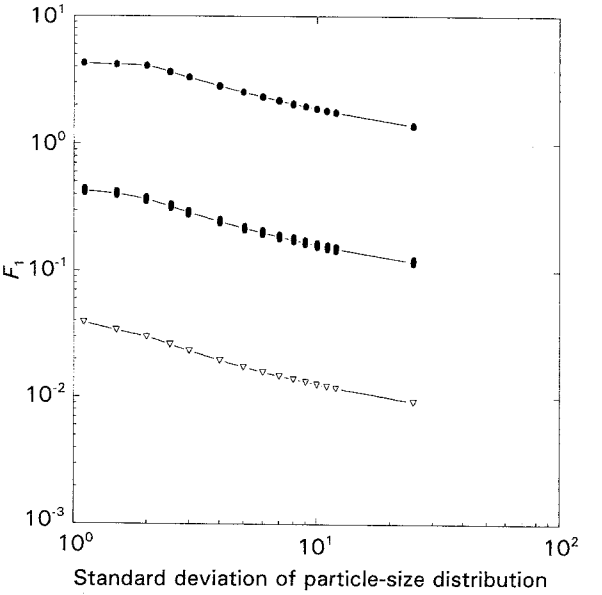

Figure 4 When grain growth occurs (in a boundary-controlled process), the rate factor, F_1, decreases when the standard deviation decreases. G_g: (●) 0.5 μm, (◖) 1.0 μm, (▽) 2.0 μm.

function of the initial particle size distribution after grain growth started. Prior to the occurrence of grain growth, the densification rate exhibits a maximum value as the initial particle-size distribution width increases. After grain growth occurs, the densification rate decreases as the initial particle-size distribution width increases.

As pointed out earlier, the use of Equation 11 ignores the presence of pores because its derivation was based on a single-phase system. However, this ignorance can be neglected for the following reason. During sintering, the migration of pores with the grain boundaries commonly occurs so that the pore–grain structure remains fixed. This is particularly true when the grain growth remains normal so that pore and boundary separation is prevented. Under this circumstance, the back stress [8, 40] or the Zener effect can be neglected for the first order of approximation. The effect of the back stress introduced by pores will be discussed later, which will show that qualitatively, the modeling results are not changed because of this back stress.

Conventional definition on sintering depicts that a sintering process consists of three stages, namely, the initial stage, the intermediate stage, and the final stage of sintering. The division of a sintering process has been due to the attempts to model sintering phenomena [42]. It was pointed out earlier in this paper that not only have few modelling works been performed for the later stages of sintering but also that grain growth was generally not considered. In addition, the border line between the initial stage and the intermediate stage is somewhat ambiguous. It was suggested that the intermediate stage of sintering occurs after the "end" of the initial stage and extends to the occurrence of a significant amount of closed porosity. During the intermediate stage of sintering, grain growth takes place. It is noted that grain growth is not a sufficient condition for the occurrence of the intermediate stage. This is not only because of the vagueness of the initiation of the intermediate stage but also due to the fact that grain-boundary migration and the resulting grain growth can begin when the porosity is sufficiently low [35]. In fact, without the consideration of grain growth, there are similarities between the models for the initial stage and most of the models for the intermediate stage, as stated earlier. Therefore, occasionally, the modelling equations of the initial stage and the intermediate stage were well used beyond the "border line" described above. Here we will divide the sintering process into two stages (1) before and (2) after the occurrence of grain growth. This is not only because of the fact stated above, but also due to the results obtained by us.

Earlier models are normally based on approximations in the geometry or diffusion flow fields due to the extremely complex geometry involved in the sintering process. A commonly used, and almost exclusively used, geometry involves two equal-sized spheres in contact. Using this geometry, the driving force, curvature ($\kappa = 1/r_\rho$), of the initial stage of sintering can be approximated. Through these approximations, some diffusion flux can then be obtained. As a result, the shrinkage rate dy/dt, for example, in the case of grain-boundary diffusion, can be expressed as [43]

$$\frac{dY}{dt} = \frac{K_7 D \gamma_s \Omega}{kT} \frac{1}{r_\rho X^2} \tag{15}$$

where X is the neck size and K_7 is a constant.

The above equation is a typical equation in "classical" sintering models. Employing the concept of these well-defined models, sintering equations for spheres with different sizes in contact can be obtained. The following expression shows such an example for the case of three spheres with different sizes in linear contact [44].

$$\frac{\Delta L}{L_0} = \frac{K_8}{G_1^{4/3}} \left\{ \left[\left(\frac{1 + R_{S_2}}{R_{S_2}^{2/3}} \right) + \left(\frac{1 + R_{S_3}}{R_{S_3}^{2/3}} \right) \right] \Big/ (2 + R_{S_2} + R_{S_3}) \right\} t^{1/3} \tag{16}$$

where K_8 is a constant, $R_{S_2} = (G_2/G_1)$, and $R_{S_3} = (G_3/G_1)$ (note that $G_3 > G_2 > G_1$). From the above equation, one can find that shrinkage depends on not only the values of R_{S_2} and R_{S_3} but also the ratio of R_{S_3} to R_{S_2}. A maximum value of the shrinkage rate can be found when proper size ratios are selected. In other words, the effects of finer and coarser particles are "competing" with each other and depend on how far apart they are from the size of the centre particle.

The contribution of particles with various sizes, i.e. a multi-component system, can be realized likewise. As finer and coarser particles are randomly added into mono-sized particles, the sintering rate changes. The opposite effects that finer and coarser particles introduce compete with each other. The resulting sintering rate depends on the size deviations of the powders added to from the mono-sized powders. For powders characterized by some distribution function $f(G)$, the effect of powders with a size falling between G and $G + \delta G$ can enter into the sintering equation as expressed by Equation 8. Because the size deviations of powders in the distribution are represented by the standard deviation, the dependence of sintering rate on the standard deviation is clear. As the standard deviation varies, the individual size deviation varies, which yields a changing sintering rate. When the competition between finer and coarser particles takes place, a maximum sintering rate will be obtained.

As sintering proceeds, grain growth occurs. During this stage, the driving force for sintering is not only the reduction of surface energy, i.e. the shrinkage of pores, but also the reduction of grain-boundary energy, i.e. elimination of grain boundaries through grain growth. The effect of particle size on sintering can be realized by considering a typical modelling microstructural feature as shown in Fig. 5 [45]. The figure illustrates that a pore is being carried along by the moving grain boundaries. The pore is surrounded by three grains with different sizes and the arrows in the figure indicate the directions of mass flow. Prior to the occurrence of grain growth, the tendency of reducing the system energy favours the diffusion of mass from all the particles to pores and, as discussed before, smaller

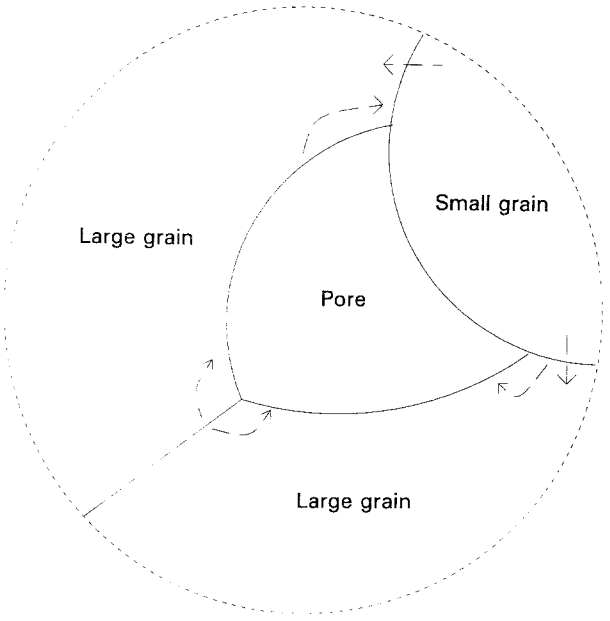

Figure 5 A pore being carried along with moving boundaries (after [45]). Arrows indicate the directions of mass flow.

particles enhance the sintering rate. The sharp curvature generated as a result of particle or grain contact prevents grain growth from occurring. However, as sintering proceeds, the tendency to reduce the system energy favours not only surface-energy reduction but also grain-boundary energy reduction. Meanwhile, pore structure could become similar to that shown in Fig. 5 when a small grain encounters two large grains.

As shown in the pore–grain structure, pore shrinkage is largely due to the mass diffusion from the large grains. At the same time, the small grain contributes much less in reducing the pore size and, as required by Equation 11, is giving away mass to the large grains to yield grain growth. As a result, the beneficial effect of small grains which can be seen in the previous stage is diminishing at this stage. On the other hand, the drawback of large grains still exists.

The effect of grain-size distribution on the sintering behaviour can also be discussed from a different angle, as follows [8]. As grain growth takes place, it is important to prevent the occurrence of abnormal grain growth. It is known that this can be prevented when the pores remain at the grain boundaries. The separation of pore and grain boundaries could occur when the grain-boundary velocity, v_b, exceeds the pore velocity, v_p. These velocities can be, respectively, expressed as in Equations 17 and 18 [44]

$$v_b = M_b\left[\alpha\gamma_b\left(\frac{1}{G_g}-\frac{1}{G}\right)-\frac{\beta N_p\gamma_b}{r}\right] \quad (17)$$

where M_b is the grain-boundary mobility, N_p is the number of pores per grain, and α and β are dimensionless constants.

$$v_p = \beta M_p\frac{\gamma_b}{r} \quad (18)$$

where M_p is the pore mobility. Therefore, the condition of interest, i.e. boundary velocity exceeding pore velocity ($v_b > v_p$), becomes

$$\left(\frac{1}{G_g}-\frac{1}{G}\right) > \frac{\beta}{\alpha r}\left(\frac{M_p}{M_b}+N_p\right) \quad (19)$$

Further analysis shows that Equation 19 can be rewritten as

$$\left(1-\frac{G_g}{G}\right) > I(P,M_b,G_g) \quad (20)$$

with

$$I(P,M_B,G_g)=\frac{\beta}{\alpha}\left(\frac{A}{M_b}\frac{P^{-(m+1)/3}}{G_g^m}+B\frac{P^{2/3}}{G_g^3}\right) \quad (21)$$

where $A = K_9(\pi/2^{1/2})^{(m+1)/3}$, $B = K_{10}(\pi/2^{1/2})^{1/3}\Omega$, m is constant depending on the diffusion path and K_9 and K_{10} are constants. It also can be shown that $A/(M_bG_g^m)$ and B/G_g^3 are of the same order of magnitude. Thus, we can plot the relative values of $I(P,M_b,G_g)$ as a function of P, as shown in Fig. 6. Also shown in this figure are several horizontal dashed lines representing various values of $(1-G_g/G)$.

Taking the middle horizontal line as an example, one can find that, during densification, pores will separate from grain boundaries at some porosity. To prevent the pore–boundary separation, one can increase the ratio of G_g/G as shown in the two lower horizontal lines. On the other hand, reducing the G_g/G ratio increases the possibility of pore–boundary separation. This clearly suggests that powders with a narrower initial particle-size distribution are preferred in obtaining high-density parts. In other words, for several powder batches with the same mean size, the one having wider initial particle-size distribution width would have a greater tendency of pore–boundary separation during grain growth. As a result, lower densification can be expected for such powders. To prevent pore–boundary separation and to ensure higher densification, powders with narrow initial particle-size distributions are required.

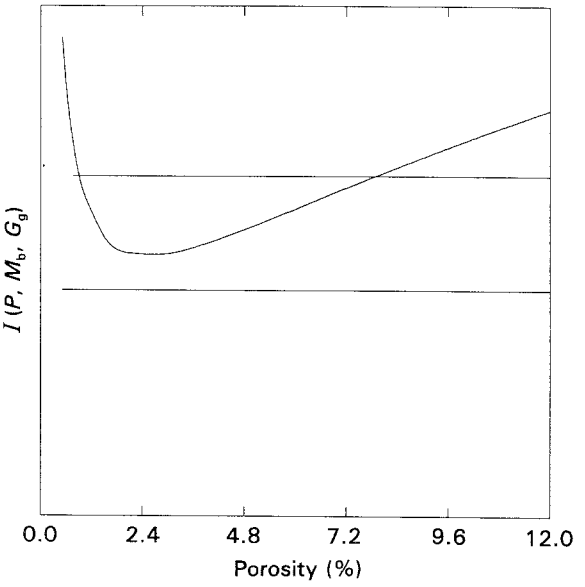

Figure 6 A plot showing the characteristic function, I, as a function of porosity. Also shown are two broken lines representing $(1 - G_g/G)$. (——) $G_g/G = 1/5$, (——) $G_g/G = 1/3$.

6. Conclusions

1. A new sintering model, taking into account the effect of starting particle-size distribution and the effect of grain growth, has been developed. The model predicts a dependence of densification on the width of starting particle-size distribution. Prior to the occurrence of grain growth, a maximum densification rate exists as the starting particle-size distribution width increases.

2. To include the effect of grain growth on densification rate, a function describing grain-growth kinetics, according to Hiller's theory, was incorporated into the modelling. During grain growth, the model predicts decreasing densification rate with increasing starting particle-size distribution width.

Acknowledgements

This work was supported by the Ohio Edison Program, Astro Met Associates, OH, and Applied Science, Inc., OH.

References

1. T.-S. YEH and M. D. SACKS, *J. Am. Ceram. Soc.* **71** (1988) C484.
2. J. S. CHAPPEL, T. A. RING and J. D. BIRCHALL, *J. Appl. Phys.* **60** (1986) 383.
3. J. P. SMITH and G. L. MESSING, *J. Am. Ceram. Soc.* **67** (1984) 238.
4. B. R. PATTERSON and L. A. BENSON, *Prog. Powder Metall.* **39** (1983) 215.
5. M. F. YAN, R. M. CANNON, U. CHOWDHRY and H. K. BOWEN, *Bull. Am. Ceram. Soc.* **56** (1977) 3.
6. W. H. RHODES, *J. Am. Ceram. Soc* **64** (1981) 19.
7. E. A. BARRINGER and H. K. BOWEN, *ibid.* **65** (1982) C 199.
8. M. F. YAN, R. M. CANNON Jr, H. K. BOWEN and U. CHOWDHRY, *Mater. Sci. Eng.* **60** (1983) 275.
9. M. D. SACKS and T.-Y. TSENG, *J. Am. Ceram. Soc.* **67** (1984) 532.
10. E. BARRINGER, N. JUBB, B. FEGLEY, R. L. POBER and H. K. BOWEN, in "Ultrastructure Processing of Ceramics, Glasses, and Composites", edited by L. L. Hench and D. R. Ulrich (Wiley Interscience, New York, 1984) pp. 568–75.
11. R. L. COBLE, *J. Am. Ceram. Soc.* **56** (1973) 461.
12. G. L. MESSING and G. Y. ONODA Jr, *ibid.* **68** (1981) 468.
13. G. C. KUZYNSKI, *Trans. AIME* **185**, (1949) 169.
14. N. CABRERA, *ibid.* **188** (1950) 667.
15. W. D. KINGERY and M. BERG, *J. Appl. Phys.* **26** (1955) 1205.
16. R. L. COBLE, *J. Am. Ceram. Soc.* **41** (1958) 55.
17. R. L. COBLE, in "Kinetics of High-Temperature Processes", edited by W. D. Kingery (Technology Press, MA and Wiley, New York, 1959) pp. 146–63.
18. G. C. KUZYNSKI, L. ABERNETHY and J. ALLAN, *ibid.*, pp. 163–71.
19. D. L. JOHNSON and I. V. CULTER, *J. Am. Ceram. Soc.* **46** (1963) 541.
20. *Idem, ibid.* **46** (1963) 545.
21. D. L. JOHNSON and T. M. CLARKE, *Acta Metall.* **12** (1964) 1173.
22. P. D. WILCOX and I. B. CULTER, *J. Am. Ceram. Soc.* **49** (1966) 249.
23. D. L. JOHNSON, *J. Appl. Phys.* **40** (1969) 192.
24. W. S. YOUNG and I. B. CULTER, *J. Am. Ceram. Soc.* **53** (1970) 659.
25. R. L. COBLE, *J. Appl. Phys.* **41** (1970) 4798.
26. D. L. JOHNSON and I. B. CULTER, in "Phase Diagrams, Materials Science and Technology, II", edited by A. M. Alper (Academic Press, New York, 1970) pp. 265–91.
27. W. R. RAO and I. B. CULTER, *J. Am. Ceram. Soc.* **55** (1972) 170.
28. R. L. COBLE, *J. Appl. Phys.* **32** (1961) 787.
29. *Idem, ibid.* **32** (1961) 793.
30. P. J. JORGENSEN, *J. Am. Ceram. Soc.* **48** (1965) 207.
31. R. L. COBLE, *ibid.* **36** (1965) 2327.
32. R. L. COBLE and T. K. GUPTA, in "Sintering and Related Phenomena", edited by G. C. Kuzynski, N. A. Hooton and C. F. Gibbon (Gordon and Breach, New York, 1967) pp. 423–41.
33. A. K. KAKAR, *J. Am. Ceram. Soc.* **51** (1968) 236.
34. T. K. GUPTA, *ibid.* **52** (1969) 166.
35. D. L. JOHNSON, *ibid.* **53** (1970) 574.
36. P. KUMAR and D. L. JOHNSON, *ibid.* **57** (1974) 65.
37. T. K. GUPTA, *ibid.* **55** (1972) 276.
38. J. H. ROSOLOWSKI and C. GRESKOVICH, *ibid.* **58** (1975) 177.
39. H. SUZUKI, *J. Appl. Phys.* **49** (1978) 4238.
40. M. HILLER, *Acta Metall.* **13** (1965) 227.
41. K. S. VENKATARAMAN and R. A. DIMILIA, *J. Am. Ceram. Soc.* **72** (1989) 33.
42. R. J. BROOK and J. H. ROSOLOSKI, in "Treatise on Solid State Sintering, 4", edited by N. B. Nannay (Plenum, New York 1976) pp. 621–69.
43. W. S. COBLENZ, J. M. DYNYS, R. M. CANNON and R. L. COBLE, in "Sintering Process", edited by G. C. Kuzynski (Gordon and Breach, New York, 1979) pp. 141–57.
44. JYH-MING TING, PhD thesis, Department of Materials Science and Engineering, University of Cincinnati, Cincinnati, OH (1991).
45. W. D. KINGERY, and B. FRANKOIS, in "Sintering and Related Phenomena", edited by G. C. Kuzynski, N. A. Hooten and C. F. Gibbon (Gordon and Breach, New York, 1967) pp. 471–98.

Received 11 May
and accepted 28 September 1993